

# 1 Temperature variability of the Iberian Range since 1602 inferred from tree-ring records

2  
3 E. Tejedor<sup>1,2,3</sup>, M.A. Saz<sup>1,2</sup>, J.M. Cuadrat<sup>1,2</sup>, J. Esper<sup>3</sup>, M. de Luis<sup>1,2</sup>

4 [1]{University of Zaragoza, 50009 Zaragoza, Spain}

5 [2]{Environmental Sciences Institute of the University of Zaragoza }

6 [3]{Department of Geography, Johannes Gutenberg University, 55099 Mainz, Germany}

7 Correspondence to: E. Tejedor (etejedor@unizar.es) 10

## 8 9 Abstract

10  
11 Tree-rings are an important proxy to understand the natural drivers of climate variability in the  
12 Mediterranean basin and hence to improve future climate scenarios in a vulnerable region. Here,  
13 we compile 316 tree-ring width series from 11 conifer sites in the western Iberian Range.  
14 We apply a new standardization method based on the trunk basal area instead of the tree  
15 cambial age to develop a regional chronology which preserves high to low frequency variability.  
16 A new reconstruction for the 1602-2012 period correlates at -0.78 with observational September  
17 temperatures with a cumulative mean of the 21 previous months over the 1945-2012  
18 calibration period. The new IR2Tmax reconstruction is spatially representative for the Iberian  
19 Peninsula and captures the full range of past Iberian Range temperature variability. Reconstructed  
20 long-term temperature variations match reasonably well with solar irradiance changes since warm  
21 and cold phases correspond with high and low solar activity, respectively. In addition, some  
22 annual temperatures downturns coincide with volcanic eruptions with a three year lag.

## 23 24 1. Introduction

25  
26 The Intergovernmental Panel on Climate Change (IPCC, 2013) highlighted a likely increase of  
27 average global temperatures in upcoming decades, and pointed particularly to the Mediterranean  
28 basin, and therefore in the Iberian Peninsula (IP), as a region of substantial modelled temperature  
29 changes. The Mediterranean area is located in the transitional zone between tropical and extra-  
30 tropical climate systems, characterized by a complex topography and high climatic variability  
31 (Hertig and Jacobeit, 2008). Taking into account these features, even relatively minor  
32 modifications of the general circulation, i.e. a shift in the location of sub-tropical high pressure  
33 cells, can lead to substantial changes in Mediterranean climate (Giorgi and Lionello, 2008),  
34 making the study area a potentially vulnerable region to anthropogenic climatic changes by  
35 anthropogenic forces, i.e. increasing concentrations of greenhouse gases (Lionello et al., 2006a)

36  
37 Major recent efforts have been made in understanding trends in temperatures throughout the  
38 IP over the instrumental period (Kenaway et al., 2012; Pena-Angulo et al., 2015; Gonzalez-  
39 Hidalgo et al., 2015) and future climate change scenarios (Sánchez et al., 2004; López-Moreno et  
40 al., 2014). However, the fact that most of the observational records do not begin until the 1950s  
41 (Gonzalez-Hidalgo et al., 2011) is limiting the possibility of investigating the inter-annual to  
42 multi-centennial long-term temperature variability. Therefore, it is crucial to explore climate  
43 proxy data and develop long-term reconstructions of regional temperature variability to evaluate  
44 spatial patterns of climatic change and the role of natural and anthropogenic forcings on climate  
45 variations (Büntgen et al., 2005). In the IP, much progress has been made to reconstruct past  
46 centuries climate variability, including analysis of documentary evidences for temperature (i.e.  
47 Camuffo et al., 2010) and droughts reconstruction (i.e. Barriendos et al., 1997; Cuadrat and  
48 Vicente, 2007; Domínguez-Castro et al., 2010). Additionally, progress has been made to further

1 understanding of long-term climate variability of the IP through dendroclimatological studies  
2 focussing on drought (Esper et al., 2014; Tejedor et al., 2015) and temperature (Büntgen et al.,  
3 2008; Dorado-Liñán et al., 2012, 2014; Esper et al., 2015a). Nevertheless, a temperature  
4 reconstruction for central Spain is still missing.

5  
6 Several studies have been made to develop a temperature reconstruction for the Iberian Range  
7 (IR, see Figure 1) using *Pinus uncinata* tree-ring data (Creus and Puigdefabreas, 1982; Ruiz,  
8 1989). The results, in fact, showed a pronounced inter-annual to century scale chronology  
9 variability. However, their main result was a complex growth response function due to a mixed  
10 climate signal instead of a temperature reconstruction. Furthermore, Saz (2003) developed a 500-  
11 year temperature reconstruction for the Ebro Depression (North of Spain), but this chronology  
12 is based on a reduced number of cores and a standardized methodology that did not retain the  
13 medium and low frequency variance.

14  
15 Here we present the first tree-ring dataset combining samples from three different sources from  
16 the eastern IR extending back from the Little Ice Age (1465) to present (2012). The aim of this  
17 study is to develop a temperature reconstruction representing the IR, and thereby fill the gap  
18 between records located in the northern and southern IP. A new methodology, based on basal area  
19 instead of the cambial-age, was applied to preserve high-to-low frequency variance in the  
20 resulting chronologies. Furthermore, the relationship between the tree-ring and climate data is  
21 reanalysed by adding memory to the climate parameters, since memory effects on tree-ring data  
22 are much less acknowledged (Anchukaitis et al., 2012). This analysis is challenging because of the  
23 mix of tree species and their unidentified responses to climate. The resulting reconstruction of  
24 September maximum temperatures over the past four centuries is compared with latest findings  
25 from the Pyrenees and Cazorla, and the relationship with solar and volcanic forcings at inter-  
26 annual to multi-decadal timescales.

## 27 28 **2 Material and methods**

### 29 30 **2.1 Site description**

31  
32 We compiled a tree ring network from 11 different sites in the western IR (Table 1) in the  
33 province of Soria. Urbión is the most extensive forest of the IP including 120,000 ha between the  
34 Burgos and Soria provinces. It has a long forest management tradition. Therefore, all sites are  
35 situated at high elevation locations where forests are least exploited and maximum tree age is  
36 reached (Fig.1). The altitude of the sampling sites ranges from 1,500 to 1,900 meters above sea  
37 level (masl) with a mean of 1,758 masl. These forests belong to the Continental Bioclimatic  
38 Belt (Guijarro, 2013) characterized by moderate mean temperatures (9.5°C, Fig.2B) and a large  
39 seasonal range including more than 90 frost days and summer heat exceeding 30°C. Mean  
40 annual precipitation for the period 1944-2014 is 927 mm (CRU TS.3 v.23 dataset by Harris et al.,  
41 2014) and reaches its maximum during December (Fig. 2AC).

42  
43 Although scotts pine (*Pinus sylvestris*) is the dominant tree species of the region, other pinaceae  
44 are found such as *Pinus pinaster*, *Pinus nigra* or *Pinus uncinata*. Especially remarkable is  
45 occurrence of *Pinus uncinata* growing above 1,900 masl and reaching its European southern  
46 distribution limits in the IR. The lithology of the study area consists of sandstones, conglomerates  
47 and lutites.

### 48 49 **2.2 Tree ring chronology development**

1  
2 The new dataset is composed by 316 tree-ring width (TRW) series of *Pinus uncinata* (56) and  
3 *Pinus sylvestris* (260) located in the western IR (Tab. 1, Fig. 1). The most recent samples were  
4 collected during the field campaign in 2013 including old dominant and co-dominant trees with  
5 healthy trunks and no sign of human interference. We extracted two core samples from each tree  
6 at breast height (1.3 m) when possible, otherwise, we try to avoid compression wood due to steep  
7 slopes, compiling a set of 96 new samples from two sites, i.e. the outermost ring is 2012. Core  
8 samples were air-dried and glued onto wooden holders and subsequently sanded to ease growth  
9 ring identification (Stokes and Smiley, 1968). The samples were then scanned and synchronized  
10 using CoRecorder software (Larsson, 2012) (Cybis Dendrochronology, 2014) to identify the  
11 position and exact dating of each ring. The tree-ring width was measured, at 0.01 mm precision,  
12 using LINTAB table (Rinn, 2005). Prior to detrending, COFECHA (Holmes, 1983) was used to  
13 assess the cross-dating of all measurement series.

14  
15 An additional set of 95 samples from three sites was provided by the project CLI96-1862 (Creus  
16 et al., 1992; Saz, 2003) i.e., the outermost rings range from 1992 to 1993. Finally, a set of 125  
17 samples from five sites was downloaded from the International Tree Ring Data Bank  
18 (ITRDB, <http://www.ncdc.noaa.gov/data-access/paleoclimatology-data/datasets/tree-ring>). These  
19 data were developed in the 1980s by K. Richter and collaborators, i.e. the outermost rings  
20 range from 1977 to 1985.

21  
22 In order to attempt a climate reconstruction for the western IR from this tree-ring network, we  
23 perform an exploratory analysis of the 11 tree-ring sites by creating a correlation matrix of the raw  
24 TRW series for each site and the correlation with a composite regional chronology. Calculations  
25 are computed for the common period (1842-1977) and for the full period (1465- 2012).

### 26 27 2.2.1 Standardization methods

28  
29 The key concept in dendroclimatology is referred to as the standardization process (Fritts,  
30 1976; Cook et al., 1990) where the aim is to preserve as much of the climate-related information  
31 as possible while removing the non-climatic information from the raw TRW measurements.  
32 However, with most of the standardization methods a varying proportion of the low-frequency  
33 climatic information is also lost in the process (Grudd, 2008). When the aim is to use tree-ring  
34 chronologies as a proxy for climatic reconstructions, an adequate standardization is critical and the  
35 best method should preserve high to low frequency variations (Büntgen et al., 2004). It is common  
36 practice to calculate a mean value function as the best estimate of the trees' signal at a site (Frank  
37 et al., 2006).

38  
39 We here applied four standardization methods to the 316 TRW measurement series to develop a  
40 single tree-ring index chronology. (i) To emphasize inter-decadal and higher frequency variations,  
41 each ring width series was fitted with a cubic spline with a 50% frequency response cut off at 67%  
42 of the series length (Cook et al., 1990). A bi-weight robust mean was calculated to assemble the  
43 ArstanSTD regional chronology. (ii) A residual chronology (ArstanRES) is produced after  
44 removing first-order autoregression to emphasize high-frequency variability. (iii) To preserve  
45 common inter-decadal and lower frequency variations, Regional Curve Standardization (RCS)  
46 was applied (Mitchell, 1967; Briffa et al., 1992, 1996; Esper et al., 2003). RCS is an age-  
47 dependent composite method and involves dividing the size of each tree-ring by the value  
48 expected from its cambial age. To assemble the chronology, all the series are aligned by cambial  
49 age. A single growth function (regional curve, RC) smoothed using a spline function of 10% of

1 the series length is fit to the mean of all age-aligned series. A biweight robust mean was applied  
2 to develop the RCS chronology (RCS). To preserve high to low frequency variance, we  
3 additionally applied a novel standardization method based on the principles of RCS. However,  
4 instead of using the cambial age of the trees as the independent variable, we used their sizes,  
5 calculated as the basal area of the tree in the year prior to ring formation. Then, a Poisson  
6 regression model was used to fit the individual tree-ring widths. Standardized indices were  
7 calculated as the ratio between the observed and predicted values, and a biweight robust mean  
8 was used to develop the Basal Area Poisson chronology (BasPois).

9  
10 To evaluate uncertainty of the mean chronologies running interseries correlations ( $R_{bar}$ ) and the  
11 express population signal (EPS) were calculated (Wigley et al., 1984).  $R_{bar}$  is a measure of the  
12 strength of the common growth 'signal' within the chronology (Wigley et al., 1984; Briffa  
13 and Jones, 1990), here calculated in a 50-year window sliding along the chronology. EPS is an  
14 estimate of the chronology's ability to represent the signal strength of a chronology on a  
15 theoretical infinite population (Wigley et al., 1984).

### 16 17 **2.3 Climatic data, calibration and climate reconstruction**

18  
19 Monthly temperature (mean, maximum, and minimum) and precipitation values from the gridded  
20 CRU TS v.3.22 dataset (0.5° resolution) dataset for the period 1945-2012 were used (Harris et  
21 al. 2014). The three grid points closest to the tree-ring network were averaged to develop a  
22 regional time series (Fig. 1). In addition, we calculate a cumulative monthly mean for each of the  
23 four parameters (max., min., mean temperature, and monthly precipitation). The cumulative mean  
24 is calculated by adding the months gradually. First the previous month is added, and then further  
25 months are included up to 36 previous months. For the calculations we take into account the  
26 current and the previous year. To indicate the climate parameter an acronym will be set as  
27 Temperature<sub>max, mean, or min\_Cumulative months\_Calendar month</sub><sup>-1, for previous year</sup>. For instance, the  
28 maximum temperature of the previous year October with 20 months of cumulative monthly mean  
29 will be referred as  $T_{max\_20\_Oct}^{-1}$ .

30  
31 For calibration, we correlated the four chronologies (ArstanSTD, ArstanRES, RCS, and BasPois)  
32 with monthly climate data and the cumulative monthly mean derived. However, to be consistent  
33 statistically, the two chronologies which highlight high frequency variations, ArstanRES and  
34 ArstanSTD, were correlated with the detrended climatic data. To assess the stability of the  
35 correlation, we calculated a 30-year moving correlation shifted along 1945-2012 with the  
36 cumulative monthly mean from the current and the previous year. In addition, the maximum and  
37 minimum differences between the moving correlations were calculated. As a result, the climatic  
38 variable chosen for the reconstruction is supported by having the highest moving correlation with  
39 the least difference between the maximum and the minimum over the moving correlation period.

40  
41 A split calibration/verification approach was perform over the periods 1945-1978 and 1979-2012  
42 to evaluate the accuracy of the transfer model considering the following metrics; Pearson's  
43 correlation ( $r$ ), coefficient of determination ( $r^2$ ), reduction of error (RE), mean square error  
44 (MSE), the sign test (Cook et al., 1994) and the Durbin-Watson test (Durbin and Watson, 1951).  $R$   
45 is a measure of the linear correlation between the chronology and climatic variable.  $R^2$  indicates  
46 how well the data fit a statistical model. An  $r^2$  of 1 indicates that the regression line perfectly fits  
47 the data; an  $r^2$  of 0 indicates that there is not fit at all. RE compares the skill of the estimated  
48 values with that obtained by using the mean value of the calibration period for every year. It is  
49 particularly useful since it checks whether a proxy is able to follow the lower frequency changes in

1 climate between the calibration and verification periods (Wahl and Amman, 2007) and hence it  
2 provides a sensitive measure of the reliability of a reconstruction (Cook et al., 1994; Akkemik et  
3 al., 2005; Büntgen et al., 2008); it ranges from +1 indicating perfect agreement, to minus infinity.  
4 MSE estimates the difference between the modelled and measured while sign test compares  
5 the number of agreeing and disagreeing interval trends, from year-to-year, between the observed  
6 and reconstructed series (Fritts et al., 1990; Cufar et al., 2008). To verify that there is no  
7 autocorrelation in the residuals we perform the Durbin-Watson test. Additionally, a Superposed  
8 Epoch Analysis (SEA; Panofsky and Brier, 1958) was performed using dplR (Bunn, 2008) to  
9 assess post-volcanic cooling signals in our reconstruction. The approach has been used in studies  
10 of volcanic effect on climate (Fischer et al., 2007; D'Arrigo et al., 2009; Esper et al., 2013a,  
11 2013b). The major volcanic events chosen for the analysis were those identified by Crowley  
12 (2000), in order of magnitude (1815, 1641, 1809, 1831, 1992, 1883, 1902, 1695, 1674 and 1783).

13  
14 To transfer the TRW chronology into a temperature reconstruction a linear regression model was  
15 used. The temperature was set as the dependent variable and the chronology as the independent  
16 variable, then, we used Ordinary Least Squares assuming Gaussian independent errors to estimate  
17 the regression coefficient. The magnitude and the spatial extent of the climate signal are evaluated  
18 considering the CRU TS v. 3.22 gridded dataset for Europe.

### 19 20 **3 Results**

21  
22 The correlation matrix (Fig. 3) shows not only the high inter-correlation between sampling sites  
23 and tree species but also the high correlation between each chronology and the regional  
24 chronology. The highest correlation is found between *Pinus uncinata* (VIN and CAV) located at  
25 the highest altitude. On the other hand, the weakest correlation is found between one of the lowest  
26 sites (s006) and the highest (VIN). The mean correlation among all sampling sites is  $r = 0.51$  over  
27 the common period (1842-1977) is 0.51, and  $r = 0.46$  over the full period of overlap, revealing a  
28 regionally common, external forcing controlling tree growth and justifying the development of a  
29 single chronology integrating the data from this IP tree-ring network.

30  
31 The model (regional curve) of the RCS standardization method and the model of the BasPois  
32 method are presented in Fig.4. BasPois model (Fig.4a) indicates a growth of 130 mm when the  
33 size of the basal area is near 0 and a growth of 8mm when it reaches the maximum basal area.  
34 RCS model (Fig.4b) presents values of 250 mm of growth when the cambial age is 0 with a  
35 gradual decline of the growth until the cambial age of 450. At cambial ages from 500 to 550 a  
36 slight increase in growth is observed most likely derived by low replication regarding trees with  
37 this ages. The four chronologies after different detrending methods are shown in Figure 6.

38  
39 Calibration of the four differently detrended mean chronologies reveals a highly negative  
40 correlation with monthly mean of daily maximum temperatures (Fig. 5). The ArstanRES  
41 chronology shows moderate correlations with previous-year September ( $r = -0.39$ ), and the  
42 ArstanSTD chronology correlates at  $r = -0.56$  with both  $T_{\max\_21\_Sept}^{-1}$  and  $T_{\max\_21\_Oct}^{-1}$ .  
43 Considering the RCS chronology, the  $T_{\max\_21\_Sept}^{-1}$  signal increases to  $r = -0.57$ . Finally, the  
44 best correlation is revealed for the BasPois chronology reaching  $r = -0.78$  with  $T_{\max\_21\_Sept}^{-1}$   
45 , which is, in fact a two year cumulative monthly mean. Even though the signals show the same  
46 seasonal patterns among the chronologies, the BasPois record always shows the highest  
47 correlations. Accordingly, we used the BasPois chronology for the calibration and reconstruction  
48 process.

49

1 The final BasPois network chronology (Fig.6) is based on 316 TRW series of *Pinus uncinata* and  
2 *Pinus sylvestris* spanning the 1465-2012 period. Since this chronology is derived from only  
3 living trees, mean chronology age increases from 47 years in 1966 to 528 in 1465. The mean  
4 sensitivity is 0.21, the first-order autocorrelation is 0.83 and the inter-series correlation  
5 ( $R_{bar}$ ) reaches 0.26. The network chronology's signal to noise ratio is 48.52, and EPS exceeds  
6 0.85 after 1602, constraining the reconstruction period to 410 years until 2012.

7  
8 The selection of the best climate parameter to develop the reconstruction is presented in the  
9 Figure 7 where correlations between -0.54 and -0.86 representing only the most significant values  
10 are shown. Four parameters reveal the highest correlations over the full calibration period;  
11  $T_{max\_22\_Oct}$ ;  $T_{max\_20\_Sept}^{-1}$ ;  $T_{max\_21\_Sept}^{-1}$ ; and  $T_{max\_21\_Oct}^{-1}$ . The stability of the correlation  
12 and therefore the consistency of the signal are tested considering the minimum difference between  
13 the maximum and minimum correlation (Fig. 7b) over the full running correlation period. The  
14 smallest difference (0.24) is reached for September of the previous year with a cumulative  
15 monthly mean of 21months. Therefore, this parameter is chosen for the climate reconstruction.  
16 According to the 30-year moving correlations, maximum values are reached from 1973-2003 ( $r$   
17 = -0.80), whereas the lowest 30-year correlation ( $r$  = -0.60) is reached from 1956-1986. In  
18 addition, the relationship between  $T_{max\_21\_Sept}^{-1}$  is spatially consistent throughout the Iberian  
19 Peninsula, reaching into southern France and northern Africa (Fig.11).

20  
21 The transfer model is validated by the high correlation ( $r$  = -0.78) and significant coefficient of  
22 determination ( $r^2=0.61$ ) over the full period 1945-2012. Through the split calibration/verification  
23 process, considering 1945-1978 and 1979-2012, the temporal robustness was tested revealing  
24 highly significant correlations for both periods ( $r^2=0.41$  and  $r^2=0.55$  respectively) and verifying  
25 the final reconstruction (Table 2 and Fig. 8). The Durbin-Watson test for the full period (1.45  
26  $p<0.0001$ ) indicates no substantial autocorrelation in the residuals. To develop the final  
27 reconstruction spanning 1602-2012, we used a lineal regression model over the full period 1945-  
28 2012 with maximum temperature of September of the previous year with a cumulative monthly  
29 mean of 21months (Eq.1), denominated IR2T<sub>max</sub>:

$$30 \quad IR2T_{max} = 3.9759 * BasPoisChron + 15.769 \quad (r^2=0.61; p < 0.0001) \quad (1)$$

### 31 **3.1 IR2T<sub>max</sub> reconstruction**

32  
33 IR2T<sub>max</sub> describes 410 years of maximum temperature of  $T_{max\_21\_Sept}^{-1}$  meaning it has memory  
34 of the last two years. Biennial temperature ranges from 13.52°C (-2.13°C with respect to the  
35 mean) in 1603 to 17.64°C (+1.94°C with respect to the mean) in 2005 (Fig. 9). It is  
36 remarkable that from 1602, 12 of the 25 warmest biennial periods happen during the 20<sup>th</sup> and  
37 21<sup>st</sup> centuries. IR2T<sub>max</sub> covers a part of the Little Ice Age (Grove, 1988) from 1602 to the end  
38 of the nineteenth century. The temperature variability is 3.92°C in the seventeenth century,  
39 2.89°C in the eighteenth century, 3.17°C in the nineteenth century and 3.07°C in the twentieth  
40 century. The seventeenth and eighteenth centuries were the coldest of the reconstruction with 73%  
41 and 80% of the biennials with temperatures below the long-term mean, respectively. On the  
42 other hand, the nineteenth and the twentieth centuries were the warmest with 66% and 78% of  
43 the biennial periods exceeding the mean.

44  
45 The main driver of the large-scale character of the warm and cold episodes may be changes in the  
46 solar activity (Fig.9). The beginning of the reconstruction starts with the end of the Spörer  
47  
48

1 Minimum. The Maunder minimum, from 1645 to 1715 (Luterbach et al., 2001) seems to cohere  
2 with a cold period from 1645 to 1706. In addition, the Dalton minimum from 1796 to 1830, is  
3 detected for the period 1810 to 1838. However, a considerably cold period from 1778 to 1798 is  
4 not in consonance with a decrease in the solar activity. Four warm periods, 1626-1637, 1800-  
5 1809, 1845-1859 and 1986-2012, have been identified to cohere with increased solar activity.  
6 Overall, the correlation between the reconstruction and the solar activity is 0.34 ( $p < 0.0001$ ), and  
7 increases to  $r = 0.49$  after 11-year low pass filtering the series, though the degrees of freedom  
8 are substantially reduced due to the increase autocorrelation.

9  
10 The SEA (Fig.10) indicates some impact of volcanic eruptions on the short-term temperature  
11 variability within the reconstruction. It shows significance ( $p < 0.05$ ) decrease in September's  
12 temperature with a lag of three years.

13  
14 Figure 11 shows the spatial correlation between the reconstruction and the CRU TS v.3.22 for  
15 Europe and northern Africa. High coefficient of determination ( $r^2 > 0.4$ ,  $p < 0.0001$ ) indicates a  
16 robust agreement and spatial extend of the reconstruction over the Iberian Peninsula (IP),  
17 especially for the central and Mediterranean Spain. The spatial correlation, however, decreases  
18 towards the southwest of the IP and the north of Europe.

#### 19 20 **4 Discussion and conclusion**

21 A novel detrending approach, considering a Basal Area-Poisson model (BasPois) instead of the  
22 traditional regional curve (Esper et al., 2003) has certainly improved the skill of the reconstruction  
23 and enabled retaining high-to-low frequency climate variance. The traditional approach of using  
24 RCS with the mean TRW curve of the age-aligned data only reached correlations with the  
25  $T_{\max\_21\_Sept}$  up to  $r = -0.57$ , while with the new approach reached  $r = -0.78$ .

26  
27 Observed improvements in the reconstruction's skills associated to the BasPois detrending  
28 approach need to be determined in other species and environmental conditions. However, several  
29 theoretical and practical advantages can be highlighted: (1) Similarly to RCS, BasPois used all  
30 individual tree-ring measurements to complete a single detrending. High but also medium and low  
31 frequency variability is then successfully preserved in the chronology in a similar way as has been  
32 described for the RCS method. (2) Removing biological trends from raw tree-ring measurements  
33 represent the key objective of the detrending processes. However, it is usually difficult to  
34 determine the extent to which the effects of environmental factors on tree growth depend on age  
35 (genetic control) and/or on size (physiological control). Recent investigations suggest that key  
36 functional processes (and therefore potential physiological constraints) on trees are more  
37 dependent on their size than on their age (Mencuccini et al., 2005; Peñuelas, 2005). Climate  
38 growth relationships have indeed demonstrated to be strongly dependent on the size of the trees,  
39 with the differences between size classes even greater than the differences found amongst age  
40 classes or even between different species (de Luis et al., 2009). Hence, the size-based  
41 standardization considered in the BasPois approach could represent a suitable alternative to age-  
42 based standardization processes (such as RCS) in order to isolate the evidence of external,  
43 climatically driven forcing of tree growth. (3) The age of the trees and subsequently, the cambial  
44 age of each individual tree-ring, it is usually not possible to be exactly determined by standard  
45 dendrochronological samples. As a consequence, age-based standardization processes should be  
46 often based on age estimations instead of directly measured values. On the contrary, the diameter  
47 at breast height (DBH) is a parameter that is routinely obtained during the dendrochronological  
48 sampling and then, the size of each tree prior to the formation of any tree-ring can be directly and  
49 unequivocally determined. (4) Finally, an additional obvious advantage is related to the

1 possibility to design a sampling strategy including trees of different size classes in order to obtain  
2 a more unbiased distribution of tree-rings in relation to the independent variable used for the  
3 detrending. To the best of our knowledge, size-based standardization processes as tested for our  
4 database have not been applied elsewhere. Further research is needed to generalize the advantages  
5 of such approach.

6  
7 According to the previously discussed novel detrending approach and based on a coherent  
8 network of 11 tree-ring sites in the IR including 316 TRW series we developed a 410-year  
9 maximum September temperature reconstruction. This record is the first climate reconstruction  
10 for the IR filling the gap between the temperature reconstructions developed for the north IP  
11 (Büntgen et al., 2008; Dorado-Liñán et al., 2012a, Esper et al., 2015a) and for the southern IP  
12 (Dorado-Liñán et al., 2014). The IR2T<sub>max</sub> has been achieved using TRW as well as for the  
13 southern IP (Dorado-Liñán et al., 2014). However, for the Pyrenees, MXD (Büntgen et al.,  
14 2008, Dorado-Liñán et al., 2012a) or stable isotopes (Esper et al., 2015a) are needed to get skillful  
15 records for a temperature reconstruction.

16  
17 The main statistics used to verify the accuracy of the reconstruction present similar values to those  
18 developed for the IP. For instance, the RE coefficient for the period 1945-2012 is 0.56 meaning  
19 that the reconstruction has indeed useful skills to develop a reconstruction. A relatively high  
20 signal to noise ratio indicates there is meaningful climatic information in the chronology. The  
21 mean correlation between sites for the common period ( $r = 0.51$ , Fig. 3) reveals substantial  
22 agreement between the sites and species. Correlation is strongest among high elevation sites  
23 including the sites VIN and CAV which are both derived from *Pinus uncinata*. The regional  
24 climate variability was retained quite accurately by the mean chronology (including 48.52 of  
25 signal to noise), which highlights the beauty of regional averages (Briffa et al., 1998).

26  
27 The original, raw chronology extended over the 1465-2012 period, some 150 years longer than the  
28 final reconstruction. However, due to low EPS values prior to 1602, which is related to the low  
29 number of samples the final reconstruction was developed for the period 1602-2012.

30  
31 In this study, we detected a maximum temperature correlation with  $T_{\max\_21\_Sept}^{-1}$  of -0.78.  
32 Nonetheless, the negative temperature correlation is already shown for the previous September  
33 ( $r=-0.56$ , with BasPoisChron) without any cumulative monthly mean. That would mean that  
34 within the environment in which trees are growing and with respect to the mean, they will grow  
35 more in cold than in hot years. This negative temperature correlation has been reported in  
36 numerous dendroclimatic studies (i.e. Büntgen et al., 2006; van der Werf et al., 2007) including  
37 the most recently developed climatic reconstruction for the Iberian Peninsula by Dorado-Liñán et  
38 al. (2014) showing a negative correlation with previous summer temperatures. One of the  
39 strengths of the results is adding the cumulative monthly mean to the climate variables which  
40 maximizes the correlation to  $r=-0.78$ .

41  
42 The development of climate parameters retaining temperature information of the past 2 years is  
43 certainly unusual and distinctive. However, memory effects in TRW data can arise from  
44 physiological processes already suggested by Schulman (1956) and Matalas (1962). Moreover, it  
45 is well known that TRW growth is conditioned by the storage of starch and sugar in parenchyma  
46 ray tissue and the remobilization of carbohydrates from root structures that were storage in  
47 previous growing seasons (Pallardy, 2010).



1 In addition, radial growth of trees is strongly conditioned by total needle biomass available in  
2 trees at the start of the growing season (Wang et al., 2012). In pine species, mean needle age range  
3 from 2 to 4 years (Pensa and Jalkanen, 2005) and the amount of needles formed is also controlled  
4 by temperature variations during the years of formation. As a consequence, effects of temperature  
5 variability occurred several years before tree-ring formation may play an important role in  
6 secondary growth (radial increment) indirectly through their direct effect in primary production  
7 (needles formation). Further research and specific experiments are however needed to confirm  
8 such influences and determine the physiological mechanisms behind a climate signal that extends  
9 back up to 21 months.

10  
11 Memory effects in TRW data have been also studied regarding the delayed response in TRW  
12 (1~5 years) to post volcanic eruptions associated with a decrease in current's year temperature  
13 (D'Arrigo et al., 2013; Esper et al., 2014). Thus, developing the two year memory IR2Tmax  
14 allowed us to maintain not only the low frequency signal, highlighting the warm and cold  
15 phases, which may be explained by the high correlation with solar activity during 410 years  
16 (0.34,  $p < 0.001$ ), but also the high frequency signal, emphasizing the memory effects of the  
17 volcanic eruptions in TRW, already studied by Briffa et al. (1998) and recently by Esper et al.  
18 (2015b). According to the SEA (Fig.9), the volcanic eruptions have a significance reduction (95%  
19 confidence) of September's temperature (-1.98°C) with a three years lag. However, the  
20 IR2Tmax is already considering the two previous year's temperature, which means the  
21 temperature decrease occurred the year after the extreme volcanic event in consistency with  
22 (Frank et al., 2007a). The stability of the signal was assessed by a 30-y moving correlation  
23 from 1945 to 2012, which shows a better correlation for the period 1979-2012 in agreement with  
24 the rise of temperatures observed for last decades which may be limiting TRW growth and  
25 therefore magnifying the climate signal. However, the relationship between the chronology and  
26 the climate parameter chosen never drops below -0.54 within the calibration period 1945-2012.  
27 The negative correlation with maximum temperature of previous September is in concordance  
28 with the values detected in Cazorla by Dorado-Liñán et al. (2014). Presumably, a continuous rise  
29 in temperatures, as suggested by the IPCC (2013), would also cause a continuous decrease in tree-  
30 ring growth.

31  
32 Even though the CRU dataset spans the 1901-2013 period, the distribution of meteorological  
33 observatories in the Iberian Range of Spain did not begin until the mid-twentieth century  
34 (Gonzalez-Hidalgo et al., 2011). In fact, the closest instrumental weather station, located in  
35 Vinuesa (Fig.1), began in 1945. However, due to the large amount of gaps in the time series, the  
36 CRU dataset was used instead for the split calibration/verification approach for the period 1945-  
37 2012. The advantages of regional climatic averages were already addressed by Blasing et al.  
38 (1981) stating that the average climatic record of the gridded dataset over the study area is  
39 representative of the regional climatic conditions, and does not reflect microclimate conditions  
40 which may be characteristic of the climatic record at a single station. Tree-ring data might  
41 therefore have more variance in common with the regionally averaged climatic record than  
42 with the climatic record of the nearest weather station. Generally, studies have shown that the  
43 measurements of MXD produce chronologies with an improved climatic signal (Briffa et al.,  
44 2002) as it was revealed for summer temperature reconstructions (Hughes et al., 1984; Büntgen et  
45 al., 2008; Matskovsky and Helama, 2014). However, based on a TRW chronology, the high  
46 correlation coefficient is remarkable for the full calibration period and the CRU dataset ( $r = -$   
47 0.78).

48

1 Throughout the IR2T<sub>max</sub> reconstruction we identified the main warm and cold phases (Maunder  
2 minimum, Dalton minimum) related with long-term temperature variability generally attributed  
3 to changes in cycles of solar activity (Lean et al., 1995; Lassen et al., 1995; Haigh et al.,  
4 2015). In addition, similar cold and warm phases are observed comparing with the Pyrenees  
5 (Büntgen et al. 2008) and Cazorla (Dorado-Liñán et al., 2014) reconstructions. However, prior  
6 to the Dalton minimum, a warm phase is detected in IR2T<sub>max</sub> and the Cazorla reconstruction  
7 although it is not present in the Pyrenees or in the Alps (Büntgen et al., 2011).

8  
9 Through the spatial extent and magnitude of the IR2T<sub>max</sub> reconstruction over Europe it can be  
10 acknowledged that the reconstruction is effective and usable for most of the Spanish Iberian  
11 Peninsula. Working especially for the central and Mediterranean IP with very high coefficient of  
12 determination ( $r^2 > 0.4$ ).

### 13 14 **Acknowledgements**

15  
16 This study was supported by the Spanish government through the projects ‘CGL2011-28255’,  
17 ‘CGL2015-69985’ and the government of Aragon throughout the Program of research groups  
18 (group Clima, Cambio Global y Sistemas Naturales, BOA 147 of 18-12-2002) and FEDER  
19 funds. Ernesto Tejedor is supported by the government of Aragon with a Ph.D. grant.  
20 Fieldwork was carried out in the province of Soria; we are most grateful to its authorities, for  
21 supporting the sampling campaign. We are thankful to Klemen Novak, Edurne Martinez, Luis  
22 Alberto Longares, and Roberto Serrano for help during fieldwork.

### 23 24 25 26 27 28 29 30 31 32 33 34 35 36 37 38 39 **References**

40 Akkemik, Ü., Da deviren., N., Aras, A.: A preliminary reconstruction (A.D. 1635–2000) of spring  
41 precipitation using oak tree rings in the western Black Sea region of Turkey. *Int. J. Biometeorol.*  
42 *49(5):297–302, 2005.*

43 Anchukaitis, K.J., Breitenmoser, P., Briffa, K.R., Buchwal, A., Büntgen, U., Cook, E.R.,  
44 D'Arrigo, R.D., Esper, J., Evans, M.N., Frank, D., Grudd, H., Gunnarson, B.E., Hughes, M.K.,

- 1 Kirilyanov, A.V., Körner, C., Krusic, P.J., Luckman, B., Melvin, T.M., Salzer, M.W., Shashkin,  
2 A.V., Timmreck, C., Vaganov, E.A., Wilson, R.J.S.: Tree rings and volcanic cooling. *Nat.*  
3 *Geosci.*, 5 (12), pp. 836-837, 2012.
- 4 Barriendos, M.: Climatic variations in the Iberian Peninsula during the late Maunder minimum  
5 (AD 1675-1715): An analysis of data from rogation ceremonies. *Holocene*, 7 (1), pp. 105-111,  
6 1997.
- 7 Blasing, T. J., D. N. Duvick, and D. C. West: Dendroclimatic calibration and verification using  
8 regionally averaged and single station precipitation data, *Tree-Ring Bulletin*, 41, 37-43, 1981.  
9 3332-z
- 10 Benedict, J. B. and Maisch, M.: The little ice age, Jean M. Grove, Methuen, London and New  
11 York, xxii + 498 pp. *Geoarchaeology*, 4: 363–365. 1989. doi:10.1002/gea.3340040406
- 12 Briffa, K.R. and Jones, P.D.: Basic chronology statistics and assessment. In: *Methods of*  
13 *Dendrochronology: Applications in the Environmental Sciences* (Eds. E.R. Cook and L.A.  
14 Kairiukstis), pp.137-152, 1990.
- 15 Briffa, K.R., Jones, P.D., Bartholin, T.S., Eckstein, D., Schweingruber, F.H., Karlén, W.,  
16 Zetterberg, P., Eronen, M.: Fennoscandian summers from ad 500: temperature changes on short  
17 and long timescales. *Clim. Dynam.*, 7 (3), pp. 111-119, 1992.
- 18 Briffa, K.R., Jones, P.D., Schweingruber, F.H., Osborn, T.J.: Influence of volcanic eruptions on  
19 Northern Hemisphere summer temperature over the past 600 years. *Nature*, 393 (6684), pp. 450-  
20 455, 1998.
- 21 Briffa, K.R., Osborn, T.J., Schweingruber, F.H., Jones, P.D., Shiyatov, S.G., Vaganov, E.A.:  
22 Tree-ring width and density data around the Northern Hemisphere: Part 1, local and regional  
23 climate signals. *Holocene*, 12 (6), pp. 737-757, 2002.
- 24 Bunn, A.G.: A dendrochronology program library in R (dplR). *Dendrochronologia* 26:115–124,  
25 2008.
- 26 Büntgen, U., Esper, J., Schmidhalter, M., Frank, D.C., Treydte, K., Neuwirth, B., Winiger, M.:  
27 Using recent and historical larch wood to build a 1300-year Valais-chronology. In: Gärtner H,  
28 Esper J, Schleser G (eds) *TRACE 2*: 85-92, 2004.

- 1 Büntgen, U., Esper, J., Frank, D.C., Nicolussi, K., Schmidhalter, M.: A 1052-year tree-ring proxy  
2 for Alpine summer temperatures. *Clim. Dynam.*, 25 (2-3), pp. 141-153, 2005.
- 3 Büntgen, U., Frank, D., Grudd, H., Esper, J.: Long-term summer temperature variations in the  
4 Pyrenees. *Clim. Dynam.*, 31 (6), pp. 615-631, 2008.
- 5 Camuffo, D., Bertolin, C., Barriendos, M., Dominguez-Castro, F., Cocheo, C., Enzi, S., Sghedoni,  
6 M., della Valle, A., Garnier, E., Alcoforado, M.-J., Xoplaki, E., Luterbacher, J., Diodato, N.,  
7 Maugeri, M., Nunes, M.F., Rodriguez, R.: 500-Year temperature reconstruction in the  
8 Mediterranean Basin by means of documentary data and instrumental observations. *Clim. Change*,  
9 101 (1), pp. 169-199, 2010.
- 10 Cook, E.R., Briffa, K., Shiyatov, S., Mazepa, V.: Tree-ring standardization and growth trend  
11 estimation. In: Cook ER, Kairiukstis LA (eds), *Methods of dendrochronology: applications in the*  
12 *environmental sciences*. Kluwer Academic Publishers, Dordrecht, pp 104–162, 1990.
- 13 Cook, E.R., Briffa, K.R., Jones, P.D.: Spatial regression methods in dendroclimatology: a review  
14 and comparison of two techniques. *Int. J. of Climatol.* 14, 379–402, 1994.
- 15 Creus, J., Puigdefabregas, J.: Climatología histórica y dendrocronología de *Pinus uncinata* R.  
16 *Cuad Investig Geográfica* 2(2):17–30, 1982.
- 17 Crowley, T.J.: Causes of climate change over the past 1000 years. *Science*, 289 (5477), pp. 270-  
18 277, 2000.
- 19 Čufar, K., de Luis, M., Eckstein, D., Kajfez-Bogataj, L.: Reconstructing dry and wet summers in  
20 SE Slovenia from oak tree-ring series. *Int. J. Biometeorol.* 52:607–615, 2008.
- 21 D'Arrigo, R., Wilson, R., Tudhope, A.: The impact of volcanic forcing on tropical temperatures  
22 during the past four centuries. *Nat. Geosci.*, 2 (1), pp. 51-56, 2009.
- 23 D'Arrigo, R., Wilson, R., Anchukaitis, K. J.: Volcanic cooling signal in tree ring temperature  
24 records for the past millennium, *J. Geophys. Res. Atmos.*, 118, 2013.
- 25 de Luis, M., Novak, K., Čufar, K., Raventós, J.: Size mediated climate-growth relationships in  
26 *Pinus halepensis* and *Pinus pinea*. *TreesStructFunct*, 23 (5), pp. 1065-1073, 2009.
- 27 Domínguez-Castro, F., García-Herrera, R., Ribera, P., Barriendos, M.: A shift in the spatial  
28 pattern of Iberian droughts during the 17th century. *Clim. Past*, 6 (5), pp. 553-563, 2010.

1 Dorado Liñán, I., Büntgen, U., González-Rouco, F., Zorita, E., Montávez, J.P., Gómez-Navarro,  
2 J.J., Brunet, M., Heinrich, I., Helle, G., Gutiérrez, E.: Estimating 750 years of temperature  
3 variations and uncertainties in the Pyrenees by tree-ring reconstructions and climate simulations.  
4 *Climate of the Past*, 8 (3), pp. 919-933, 2012.

5 Dorado Liñán, I., Zorita, E., González-Rouco, J.F., Heinrich, I., Campello, F., Muntán, E.,  
6 Andreu-Hayles, L., Gutiérrez, E.: Eight-hundred years of summer temperature variations in the  
7 southeast of the Iberian Peninsula reconstructed from tree rings. *Clim. Dynam.*, 44 (1-2), pp. 75-  
8 93, 2014.

9 Durbin, J., Watson, G. S.: Testing for Serial Correlation in Least Squares Regression, II. 16  
10 *Biometrika* 38 (1-2): 159-179, 1951.

11 El Kenawy, A., López-Moreno, J.I., Vicente-Serrano, S.M.: Trend and variability of surface air  
12 temperature in northeastern Spain (1920-2006): Linkage to atmospheric circulation. *Atmos. Res.*,  
13 106, pp. 159-180, 2012.

14 Esper, J., Cook, E.R., Krusic, P.J., Peters, K., Schweingruber, F.H.: Tests of the RCS method for  
15 preserving low-frequency variability in long tree-ring chronologies. *Tree-Ring Research* 59, 81-  
16 98, 2003.

17 Esper, J., Büntgen, U., Luterbacher, J., Krusic, P.: Testing the hypothesis of post-volcanic missing  
18 rings in temperature sensitive dendrochronological data. *Dendrochronologia* 13, 216-222, 2013.

19 Esper, J., Schneider, L., Krusic, P.J., Luterbacher, J., Büntgen, U., Timonen, M., Sirocko, F.,  
20 Zorita, E.: European summer temperature response to annually dated volcanic eruptions over the  
21 past nine centuries. *B. Volcanol.* 75, 2013.

22 Esper, J., DÜthorn, E., Krusic, P., Timonen, M., Büntgen, U.: Northern European summer  
23 temperature variations over the Common Era from integrated tree-ring density records. *J. Quat.*  
24 *Sci.* 29, 487-494, 2014

25 Esper, J., Großjean, J., Camarero, J.J., García-Cervigón, A.I., Olano, J.M., González-Rouco, J.F.,  
26 Domínguez-Castro, F., Büntgen, U.: Atlantic and Mediterranean synoptic drivers of central  
27 Spanish juniper growth. *Theor. and Appl. Climatol.*, 2014.

28 Esper, J., Konter, O., Krusic, P., Saurer, M., Holzkämper, S., Büntgen, U.: Long-term summer  
29 temperature variations in the Pyrenees from detrended stable carbon isotopes. *Geochronometria*  
30 42, 53-59, 2015.

- 1 Esper, J., Schneider, L., Smerdon, J.E., Schöne, B.R., Büntgen, U.: Signals and memory in tree-  
2 ring width and density data. *Dendrochronologia*, 35, pp. 62-72, 2015b.
- 3 Fischer, E.M., Luterbacher, J., Zorita, E., Tett, S.F.B., Casty, C., Wanner, H.: European climate  
4 response to tropical volcanic eruptions over the last half millennium, *Geophys. Res. Lett.*, 34,  
5 L05707, 2007.
- 6 Frank, D., Esper, J., Cook, E.R.: On variance adjustments in tree-ring chronology development.  
7 In: Heinrich I et al. (Eds.) *Tree rings in archaeology, climatology and ecology*, TRACE, Vol. 4,  
8 56-66, 2006.
- 9 Frank, D., Büntgen, U., Böhm, R., Maugeri, M., Esper, J.: Warmer early instrumental  
10 measurements versus colder reconstructed temperatures: shooting at a moving target. *Quat. Sci.*  
11 *Rev.* 26, 3298-3310, 2007a.
- 12 Fritts, H.C., Guiot, J., Gordon, G.A., Schweingruber, F.H.: Methods of calibration, verification,  
13 and reconstruction. In *Methods of Dendrochronology*, 1990.
- 14 Fritts, H.C.: *Tree rings and climate*. Academic Press, London, 1976.
- 15 Giorgi, F., Lionello, P.: Climate change projections for the Mediterranean region, *Glob. Planet.*  
16 *Change*, Volume 63, Issues 2–3, September, Pages 90-104, 2008.
- 17 González-Hidalgo, J.C., Brunetti, M., de Luis, M.: A new tool for monthly precipitation analysis  
18 in Spain: MOPREDAS database (monthly precipitation trends December 1945 November 2005).  
19 *Int. J. Climatol.*, 31 (5), pp. 715-731, 2011.
- 20 Gonzalez-Hidalgo, J.C., Peña-Angulo, D., Brunetti, M., Cortesi, N. MOTEDAS: A new monthly  
21 temperature database for mainland Spain and the trend in temperature (1951-2010).  
22 *Int. J. Climatol.*, 2015.
- 23 Grudd, H.: Torneträsk tree-ring width and density ad 500-2004: A test of climatic sensitivity and a  
24 new 1500-year reconstruction of north Fennoscandian summers. *Clim. Dynam.*, 31 (7-8), pp. 843-  
25 857, 2008.
- 26 Guijarro, J.A.: Tendencias de la temperatura en España. En García Legaz, C. y Valero, C.  
27 (Coords). *Fenómenos meteorológicos adversos en España*. AEMET y CCS. Madrid, 2013.
- 28 Haigh, J.D., Cargill, P.: *The Sun's Influence on Climate*, pp. 1-207, 2015.

1 Harris, I., Jones, P.D., Osborn, T.J., Lister, D.H.: Updated high-resolution grids of monthly  
2 climatic observations - the CRU TS3.10 Dataset. *Int. J. Climatol.*, 34 (3), pp. 623-642, 2014.

3 Hertig, E. and J. Jacobeit: Assessments of Mediterranean precipitation changes for the 21st  
4 century using statistical downscaling techniques. *Int. J.Climatol.* 28(8): 1025-1045, 2008.

5 Holmes, R.L.: Computer-assisted quality control in tree-ring dating and measurement. *Tree-Ring*  
6 *Bull* 43:69–78, 1983.

7 Hughes, M.K., Schweingruber, F.H., Cartwright, D., Kelly, P.M.: July-August temperature at  
8 Edinburgh between 1721 and 1975 from tree-ring density and width data. *Nature*, 308 (5957), pp.  
9 341-344, 1984

10 IPCC, 2013: *Climate Change 2013: The Physical Science Basis. Contribution of Working Group I*  
11 *to the Fifth Assessment Report of the Intergovernmental Panel on Climate Change* [Stocker, T.F.,  
12 D. Qin, G.-K. Plattner, M. Tignor, S.K. Allen, J. Boschung, A. Nauels, Y. Xia, V. Bex and P.M.  
13 Midgley (eds.)]. Cambridge University Press, Cambridge, United Kingdom and New York, NY,  
14 USA, 1535 pp, doi:10.1017/CBO9781107415324.

15 Larsson, L.A.: CoRecorder&CDendro program. Cybis Elektronik & Data AB. Version 7.6, 2012.

16 Lassen, K., Friis-Christensen, E.: Variability of the solar cycle length during the past five  
17 centuries and the apparent association with terrestrial climate. *J. Atmos. Sol.-Terr. Phys* , 57 (8),  
18 pp. 835-845, 1995.

19 Lean, J., Beer, J., Bradley, R.: Reconstruction of solar irradiance since 1610: implications for  
20 climate change. *Geophys. Res. Lett*, 22 (23), pp. 3195-3198, 1995.

21 Lionello, P., Malanotte-Rizzoli, P., Boscolo, R., Alpert, P., Artale, V., Li, L., Luterbacher, J.,  
22 May, W., Trigo, R., Tsimplis, M., Ulbrich, U., Xoplaki, E.: The Mediterranean climate: An  
23 overview of the main characteristics and issues. *Developments in Earth and Environmental*  
24 *Sciences*, 4 (C), pp. 1-26, 2006a.

25 López-Moreno, J.I., El-Kenawy, A., Revuelto, J., Azorín-Molina, C., Morán-Tejeda, E., Lorenzo-  
26 Lacruz, J., Zabalza, J., Vicente-Serrano, S.M.: Observed trends and future projections for winter  
27 warm events in the Ebro basin, northeast Iberian Peninsula. *Int.l J. Climatol.*, 34 (1), pp. 49-60,  
28 2014.

1 Luterbacher, J., Rickli, R., Xoplaki, E., Tinguely, C., Beck, C., Pfister, C., Wanner, H.: The Late  
2 Maunder Minimum (1675-1715) - A key period for studying decadal scale climatic change in  
3 Europe. *Clim. Change*, 49 (4), pp. 441-462, 2001.

4 Luterbacher, J., Xoplaki, E., Casty, C., Wanner, H., Pauling, A., Küttel, M., Rutishauser, T.,  
5 Brönnimann, S., Fischer, E., Fleitmann, D., Gonzalez-Rouco, F.J., García-Herrera, R., Barriendos,  
6 M., Rodrigo, F., Gonzalez-Hidalgo, J.C., Saz, M.A., Gimeno, L., Ribera, P., Brunet, M., Paeth,  
7 H., Rimbu, N., Felis, T., Jacobeit, J., Dünkeloh, A., Zorita, E., Guiot, J., Türke, M., Alcoforado,  
8 M.J., Trigo, R., Wheeler, D., Tett, S., Mann, M.E., Touchan, R., Shindell, D.T., Silenzi, S.,  
9 Montagna, P., Camuffo, D., Mariotti, A., Nanni, T., Brunetti, M., Maugeri, M., Zerefos, C., Zolt,  
10 S.D., Lionello, P., Nunes, M.F., Rath, V., Beltrami, H., Garnier, E., Ladurie, E.L.R.: Chapter 1  
11 Mediterranean climate variability over the last centuries: A review, 2006.

12 Matalas, N.C.: Statistical properties of tree ring data. *Hydrol. Sci. J.* 7, 39–47, 1962.

13 Matskovsky, V.V., Helama, S.: Testing long-term summer temperature reconstruction based on  
14 maximum density chronologies obtained by reanalysis of tree-ring data sets from northernmost  
15 Sweden and Finland. *Clim.Past* 10, 1473–1487, 2014.

16 Mencuccini, M., Martínez-Vilalta, J., Vanderklein, D., Hamid, H.A., Korakaki, E., Lee, S.,  
17 Michiels, B.: Size-mediated ageing reduces vigour in trees. *Ecol. Lett.*, 8 (11), pp. 1183-1190,  
18 2005.

19 Mitchell, V.L.: An investigation of certain aspects of tree growth rates in relation to climate in the  
20 central Canadian boreal forest. Technical report 33pp. Department of Meteorology, University of  
21 Wisconsin, 1967.

22 Pallardy, S.G.: *Physiology of Woody Plants*. Academic Press, 2010.

23 Panofsky, H.A., Brier, G.W.: *Some applications of statistics to meteorology*. University Park,  
24 Pennsylvania, p. 224, 1958.

25 Pena-Angulo, D., Cortesi, N., Brunetti, M., González-Hidalgo, J.C.: Spatial variability of  
26 maximum and minimum monthly temperature in Spain during 1981–2010 evaluated by  
27 correlation decay distance (CDD). *Theor. and Appl. Climatol.*, 122 (1-2), pp. 35-45, 2015.

28 Pensa, M. and R. Jalkanen: Variation in needle longevity is related to needle-fascicle production  
29 rate in *Pinus sylvestris*. *Tree Physiology* 25, 1265–1271, 2005.

30 Peñuelas, J.: Plant physiology—a big issue for trees. *Nature*, 437:965–966, 2005.



- 1 Rinn, F.: TSAPWinTM – Time series analysis and presentation for dendrochronology and related  
2 applications, Version 4.69, 2005.
- 3 Ruiz, P.: Análisis dendroclimático de *Pinus uncinata Ramond* en la Sierra Cebollera (Sistema  
4 Ibérico). Cuadernos de Investigación Geográfica 15(1-2): 75-80, 1989.
- 5 Ruiz-Flaño, P.: Dendroclimatic series of *Pinus uncinata* R. in the Central Pyrenees and in the  
6 Iberian System. A comparative study. Pirineos 132:49–64, 1988.
- 7 Sánchez, E., Gallardo, C., Gaertner, M.A., Arribas, A., Castro, M.: Future climate extreme events  
8 in the Mediterranean simulated by a regional climate model: A first approach. Glob. Planet.  
9 Change, 44 (1-4), pp. 163-180, 2004.
- 10 Saz, M.A.: Análisis de la evolución del clima en la mitad septentrional de España desde el siglo  
11 XV a partir de series dendroclimáticas. Servicio de Publicaciones de la Universidad de Zaragoza,  
12 Zaragoza, 1105 pp, 2003.
- 13 Schulman, E.: Dendroclimatic Changes in Semiarid America. Tucson, University of Arizona  
14 Press, pp. 142, 1956.
- 15 Smith, J. G. and Weston, H. K.: Nothing particular in this year's history, J. Oddball Res., 2, 14-  
16 15, 1954.
- 17 Stokes, M.A., Smiley, T.L.: An introduction to tree-ring dating, 2<sup>nd</sup> edn. The University of  
18 Arizona Press, Tucson, 1968.
- 19 Tejedor, E., de Luis, M., Cuadrat, J.M., Esper, J., Saz, M.Á.: Tree-ring-based drought  
20 reconstruction in the Iberian Range (east of Spain) since 1694. Int. J. of Biometeorol., 12 p, 2015.
- 21 Van der Werf, G.W., Sass-Klaassen, U., Mohren, G.M.J.: The impact of the 2003 summer drought  
22 on the intra-annual growth pattern of beech (*Fagus sylvatica* L.) and oak (*Quercus robur* L.) on a  
23 dry site in the Netherlands, Dendrochronologia, Volume 25, Issue 2, Pages 103-112, 2007.
- 24 Vicente-Serrano, S.M. and Cuadrat, J.M.: North Atlantic oscillation control of droughts in north-  
25 east Spain: Evaluation since 1600 A.D. Clim. Change, 85 (3-4), pp. 357-379, 2007.
- 26 Wang, F., Letort, V., Lu, Q., Bai, X., Guo, Y., de Reffye, P., and Li, B.: A Functional and  
27 Structural Mongolian Scots Pine (*Pinus sylvestris* var. *mongolica*) Model Integrating Architecture,  
28 Biomass and Effects of Precipitation. PLoS ONE 7(8): e43531, 2012.

1 Wahl, E.R. and C.M., Ammann: Robustness of the Mann, Bradley, Hughes reconstruction of  
2 Northern Hemisphere surface temperatures: examination of criticisms based on the nature and  
3 processing of proxy climate evidence. *Clim. Change* 85: 33–69, 2007.

4 Wigley, T.M.L., Briffa, K., Jones, P.D.: On the average value of correlated time series, with  
5 applications in dendroclimatology and hydrometeorology. *J. Clim. Appl. Meteorol.*, 23:201–213,  
6 1984.

7

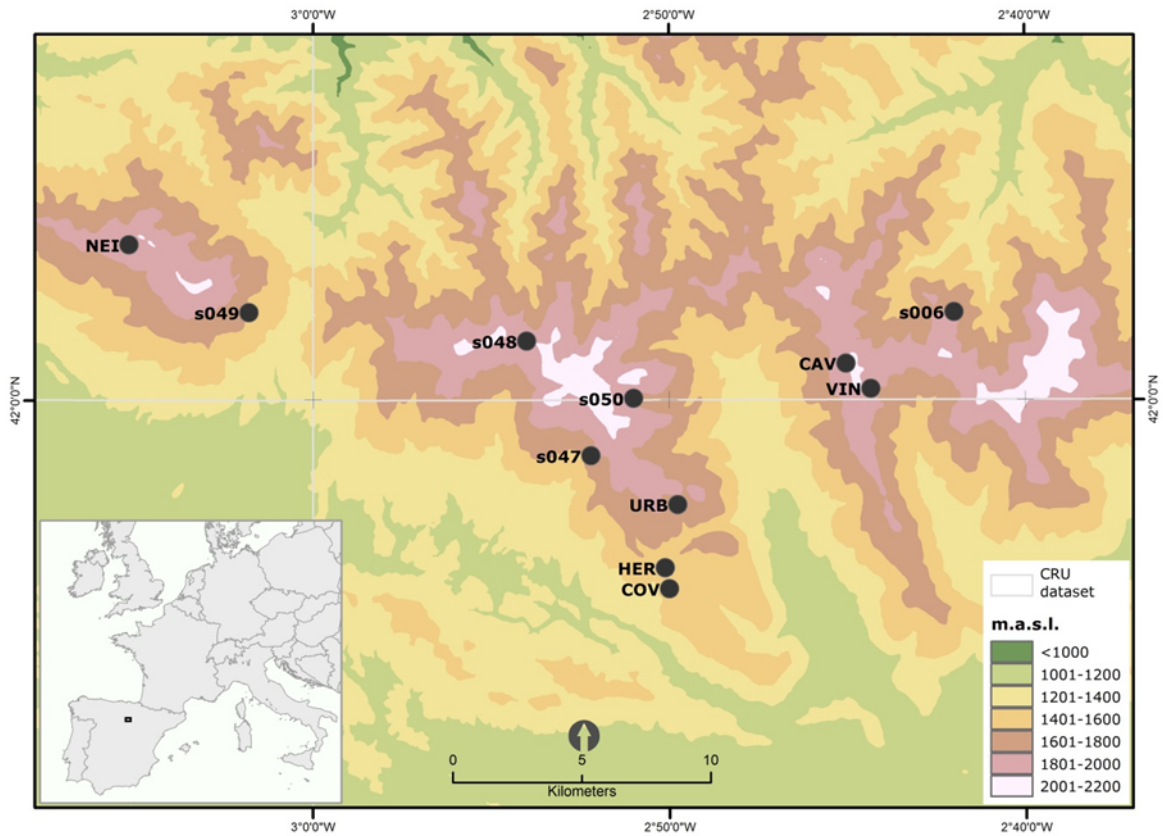
8

1 Table 1. Tree ring sites characteristics

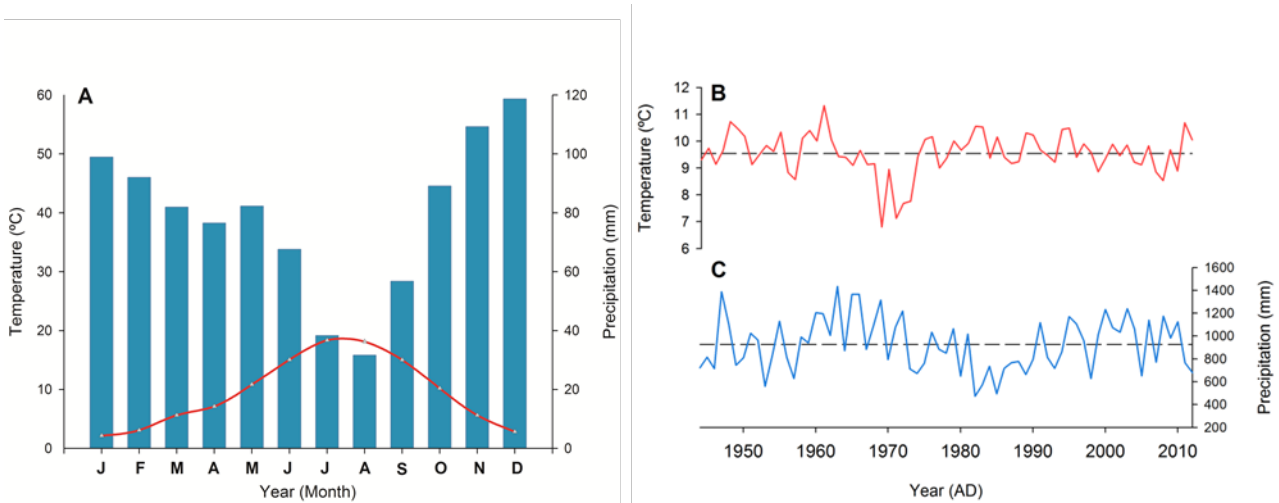
Code	Site	Source	Lat	Long	Elevation	Species	Tree no	Sample no	Tree- rings	Period
s047	Urbión Covaleda	ITRDB	41.98	-2.87	1750	PISY	15	31	6549	1567- 1983
s048	Urbión Duruelo	ITRDB	42.02	-2.90	1840	PISY	8	17	3590	1671- 1983
s049	Urbión Quintenar	ITRDB	42.03	-3.03	1840	PISY	12	27	4713	1593- 1985
s050	Urbión Vinuesa	ITRDB	42.00	-2.85	1750	PISY	4	8	1942	1681- 1983
s006	Urbión	ITRDB	42.03	-2.7	1634	PISY	11	22	2397	1842- 1977
CAV	Castillo de Vinuesa	UNIZAR	42.01	-2.75	1900	PIUN	18	36	9236	1593- 2012
COV	Covaleda	IPE- CSIC- UNIZAR	41.93	-2.83	1500	PISY	16	48	14696	1568- 1993
HER	Barranco de las heridas	IPE- CSIC- UNIZAR	41.94	-2.84	1500	PISY	25	32	9347	1562- 1993
NEI	Neila	IPE- CSIC- UNIZAR	42.05	-3.08	1850	PISY	9	15	4822	1587- 1992
URB	Picos de Urbión	UNIZAR	41.96	-2.82	1750	PISY	28	60	11328	1733- 2012

VIN	Castillo de Vinuesa	IPE-CSIC-UNIZAR	42.03	-2.73	1900	PIUN	13	20	7653	1465-1992	
Total							159	316	76273		

1 UNIZAR University of Zaragoza, IPE-CSIC Spanish National Research Council, ITRDB International Tree-Ring  
2 Databank

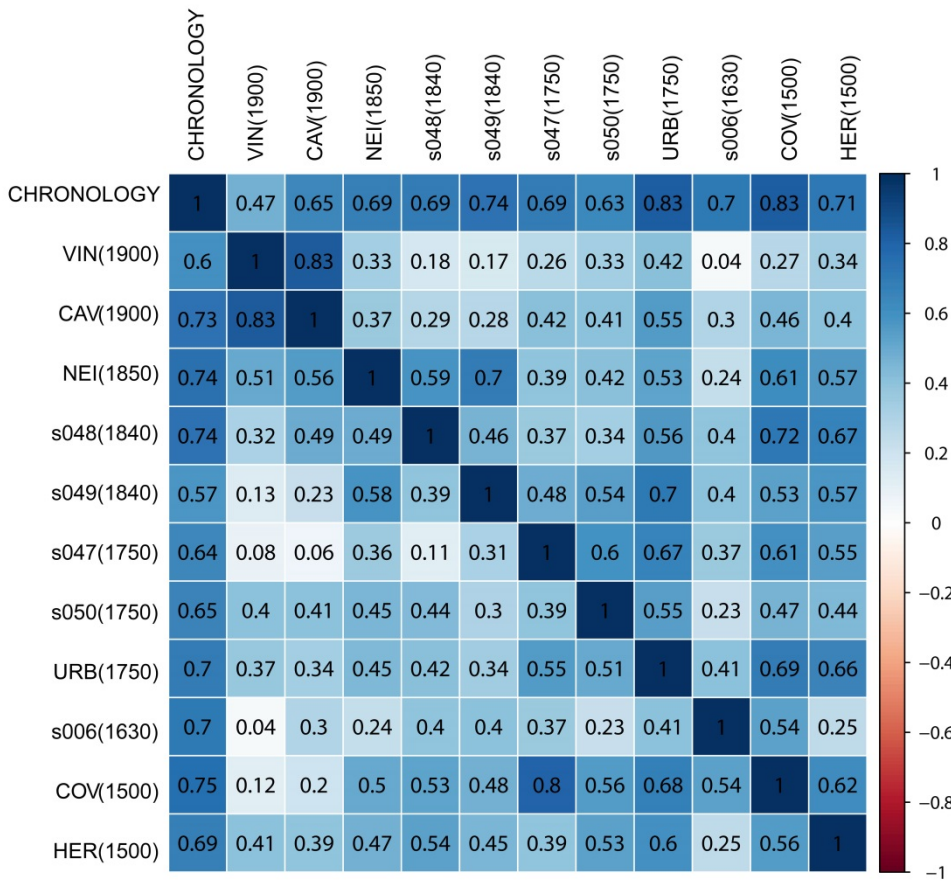


3  
4 Figure 1. Map showing the tree ring study sites and the climate data (CRU TS v.3.22) grid points  
5 in the Western Iberian Range (Soria).  
6  
7  
8  
9



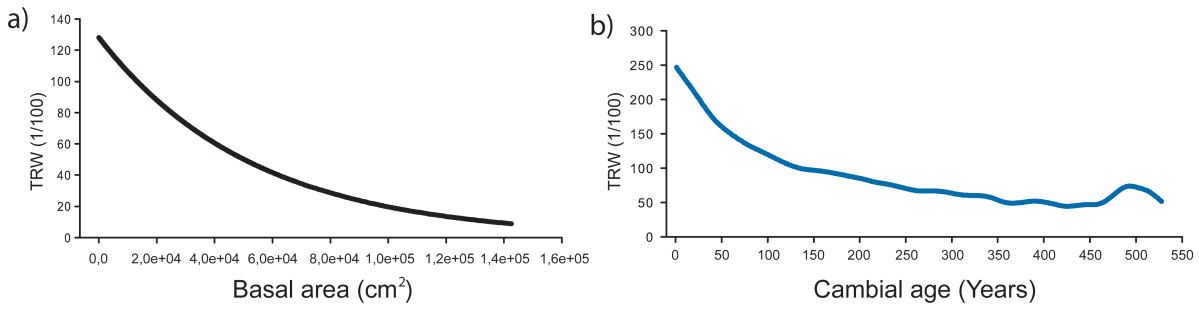
1

2 Figure 2. Climate diagram (A), mean temperature (B), mean precipitation (C) calculated using  
 3 data from CRU TS v.3.22 over the period 1944-2012 (Harris et al 2014).



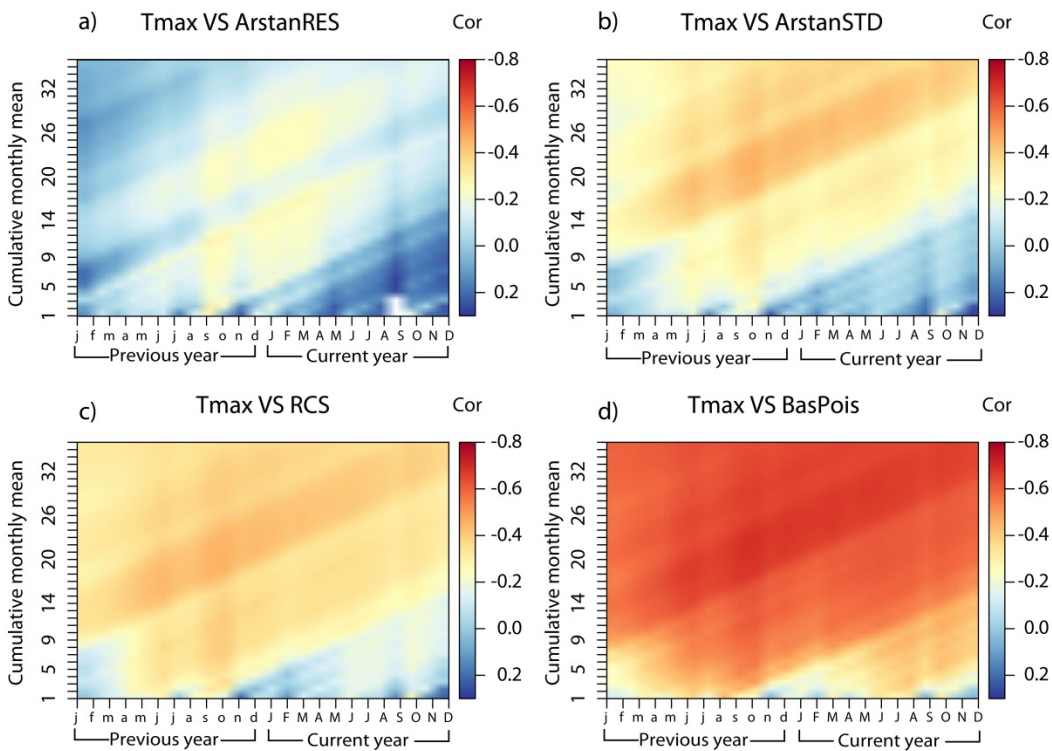
4

5 Figure 3. Correlation of the raw chronologies sorted by elevation. Top right shows the correlations  
 6 calculated over the common period 1842-1977. Bottom left shows the correlation over the full  
 7 period of overlap between pairs of chronologies



1

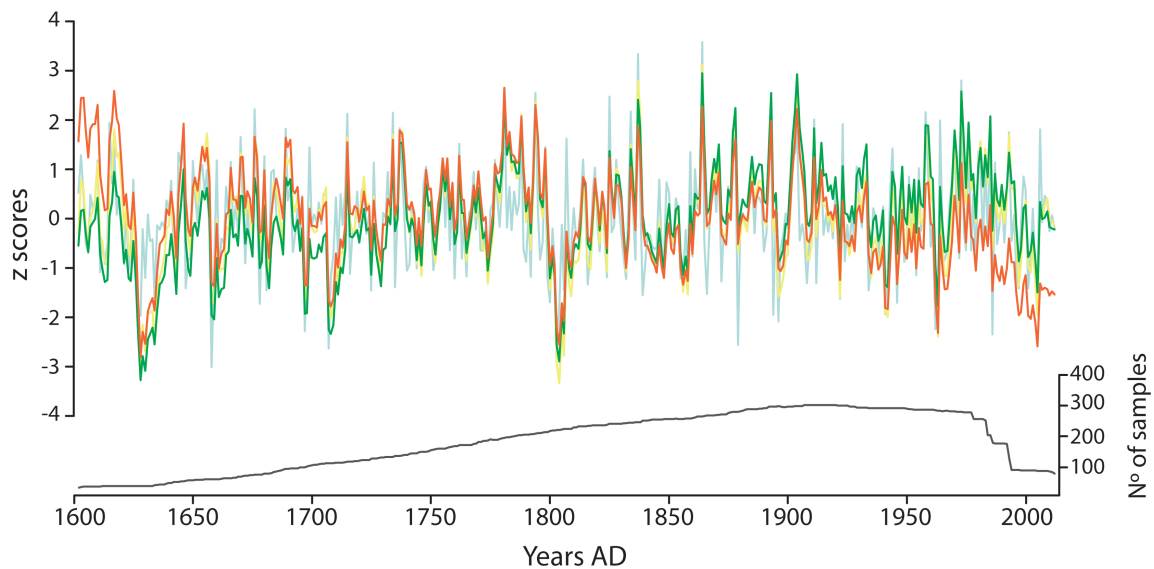
2 Figure 4. a) Represents the model of the BasPois method, b) represents the regional curve of the  
 3 RCS method.



4

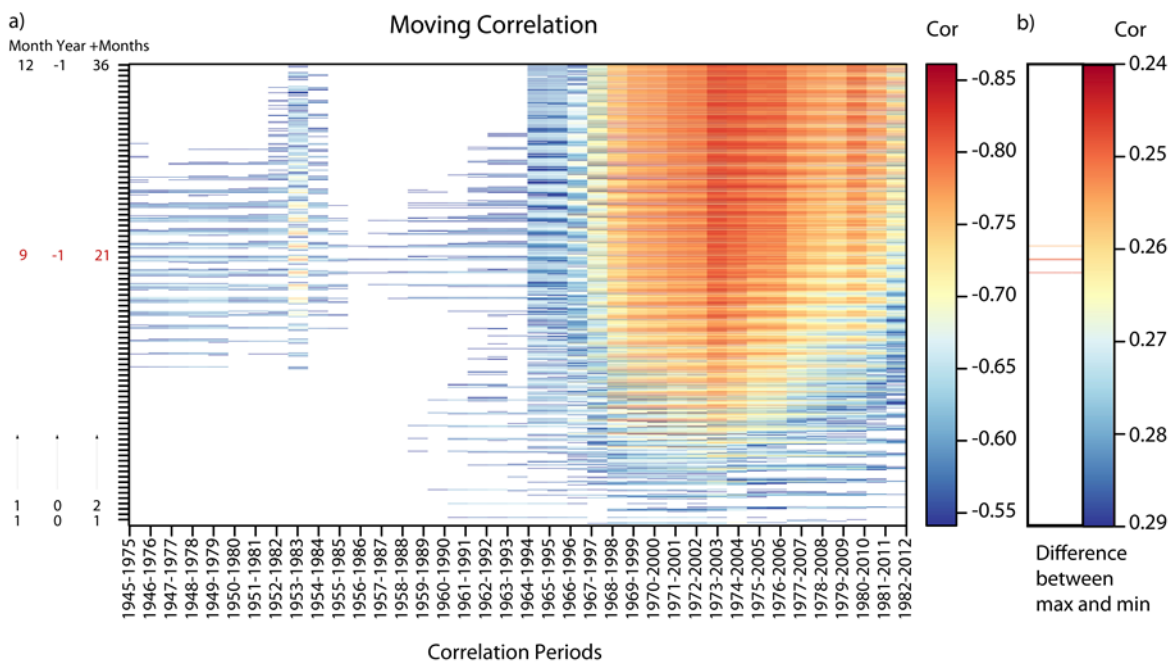
5 Figure 5. Correlation between the monthly mean of daily maximum temperature (from January of  
 6 the previous year to December of the current year with a cumulative monthly mean from 1 to 36  
 7 months) and the residual Arstan chronology (a), the standard Arstan chronology (b), the RCS  
 8 standard chronology (c) and the Basal Area-Poisson standard chronology (d).

9



1

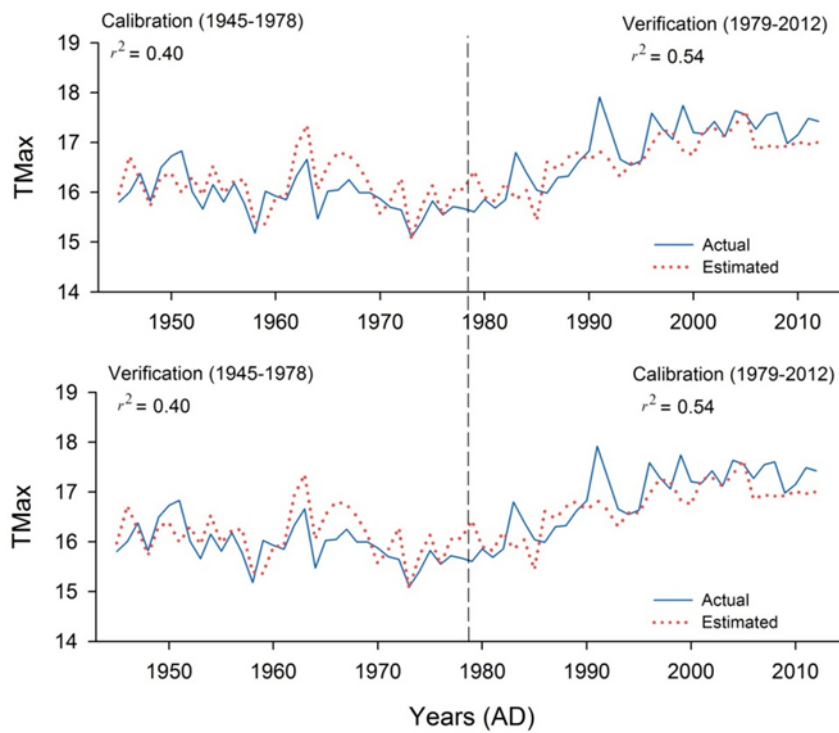
2 Figure 6. The four chronologies after different detrending methods for the  $EPS > 0.85$  period;  
 3 BasPois chronology (in orange), RCS chronology (in green), ArstanSTD chronology (in yellow),  
 4 ArstanRES chronology (in blue) and number of samples (in black)..



5

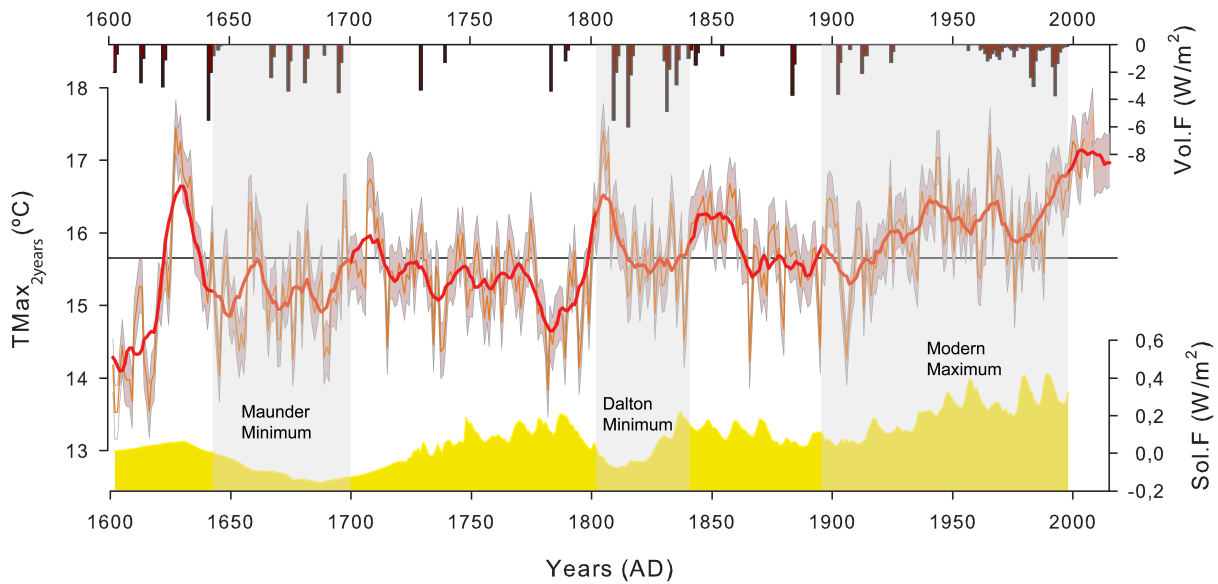
6 Figure 7.a) 30-year moving correlation from 1945 to 2012 between the monthly mean of daily  
 7 maximum temperature, from January of the current year (1,0,1) to December of the previous year  
 8 (12, -1, 36) with a cumulative monthly mean from 1 to 36 months and the BasPois chronology.  
 9 Red numbers indicates the chosen climatological parameter; 9, September, -1, previous year, 21,

1 months used for the cumulative monthly mean. b) The four best parameters are represented.  
2 Reddish line indicates the least difference between the maximum and minimum correlation in the  
3 correlation periods.



20 Figure 8. Calibration and verification results of the CRU data based Tmax<sub>Sep-1</sub> reconstruction





1 Figure 9. IR2T<sub>max</sub> reconstruction since AD 1602 for the Iberian Range. Bold red curve is an 11-  
 2 year running mean, grey shading indicates the mean square error based on the calibration period  
 3 correlation. Yellow shading at the bottom shows solar forcing and bars on top indicate volcanic  
 4 forcings (Crowley, 2000).

5

	Calibration 1945-1978	Verification 1978-2012	Calibration 1979-2012	Verification 1945-1978	Period 1945-2012
Years	34	34	34	34	68
Correlation	-0.64	0.73	-0.74	0.64	-0.78
R <sup>2</sup>	0.41	0.55	0.55	0.41	0.61
MSE	0.43	0.42	0.42	0.43	0.43
Reduction of error	0.40	0.65	0.65	0.40	0.56
Sing test	28+/6-	24+/10-	28+/6-	24+/10-	52+/16-
Durbin- Watson	1.31 p<0.01	1.53 p<0.05	1.53 p<0.05	1.31 p<0.01	1.45 p<0.001

6

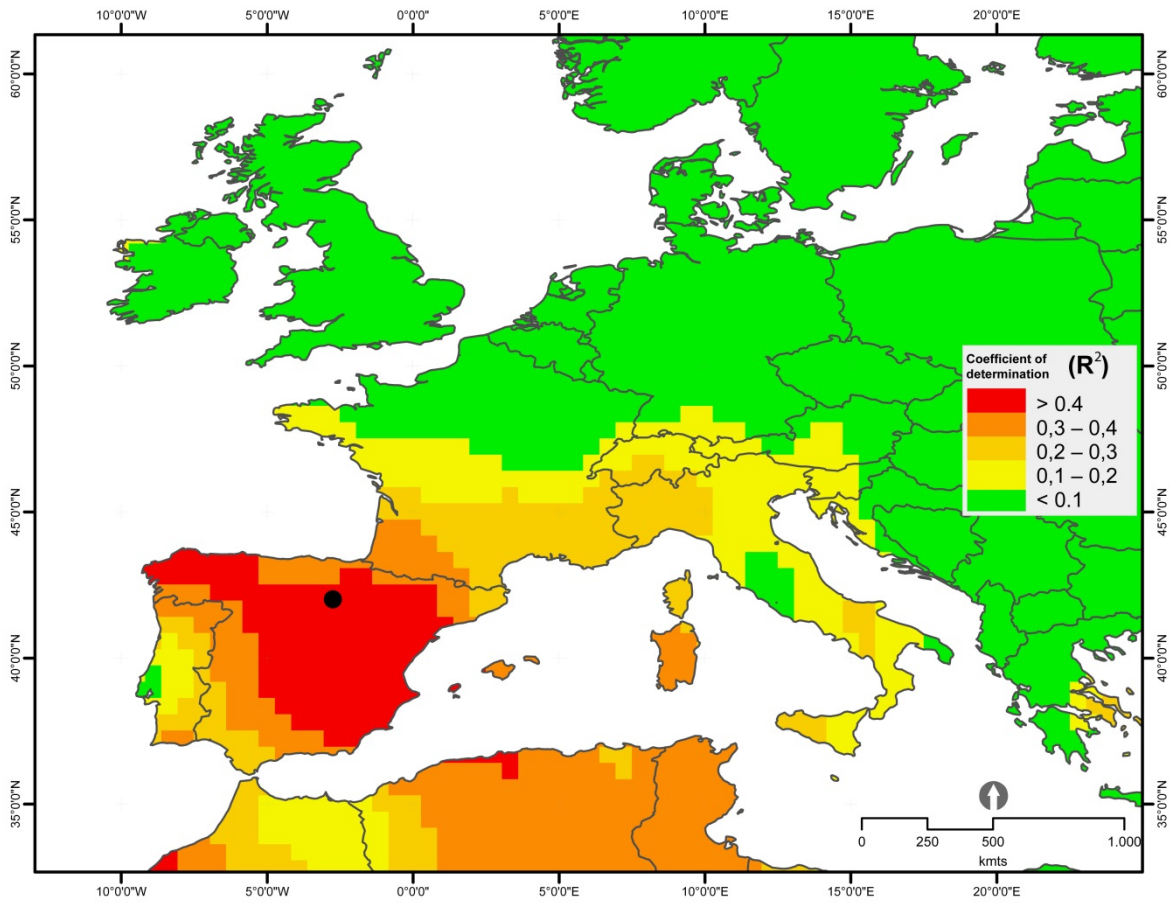
7 Table 2. Calibration/verification statistics of the IR2T<sub>max</sub> reconstruction

8

9

1  
2  
3  
4  
5  
6  
7  
8  
9

Figure 10. Superposed epoch analysis with a back and forward lag of 5 years. Significance ( $p < 0.05$ ) at 3 years after the extreme volcanic events identified in Crowley (2000).



10

Figure 11. Map showing the spatial correlation patterns of the BasPois chronology with the gridded  $T_{\max\_21\_Sept}^{-1}$ . Correlation values are significant at  $p < 0.0001$ .

13